

Constraining global air-sea gas exchange for CO₂ with recent bomb ¹⁴C measurements

Colm Sweeney,¹ Emanuel Gloor,² Andrew R. Jacobson,¹ Robert M. Key,³
Galen McKinley,⁴ Jorge L. Sarmiento,³ and Rik Wanninkhof⁵

Received 28 June 2006; revised 20 October 2006; accepted 27 November 2006; published 23 May 2007.

[1] The ¹⁴CO₂ released into the stratosphere during bomb testing in the early 1960s provides a global constraint on air-sea gas exchange of soluble atmospheric gases like CO₂. Using the most complete database of dissolved inorganic radiocarbon, DI¹⁴C, available to date and a suite of ocean general circulation models in an inverse mode we recalculate the ocean inventory of bomb-produced DI¹⁴C in the global ocean and confirm that there is a 25% decrease from previous estimates using older DI¹⁴C data sets. Additionally, we find a 33% lower globally averaged gas transfer velocity for CO₂ compared to previous estimates (Wanninkhof, 1992) using the NCEP/NCAR Reanalysis 1 1954–2000 where the global mean winds are 6.9 m s⁻¹. Unlike some earlier ocean radiocarbon studies, the implied gas transfer velocity finally closes the gap between small-scale deliberate tracer studies and global-scale estimates. Additionally, the total inventory of bomb-produced radiocarbon in the ocean is now in agreement with global budgets based on radiocarbon measurements made in the stratosphere and troposphere. Using the implied relationship between wind speed and gas transfer velocity $k_s = 0.27 \langle u_{10}^2 \rangle (Sc/660)^{-0.5}$ and standard partial pressure difference climatology of CO₂ we obtain an net air-sea flux estimate of 1.3 ± 0.5 PgCyr⁻¹ for 1995. After accounting for the carbon transferred from rivers to the deep ocean, our estimate of oceanic uptake (1.8 ± 0.5 PgCyr⁻¹) compares well with estimates based on ocean inventories, ocean transport inversions using ocean concentration data, and model simulations.

Citation: Sweeney, C., E. Gloor, A. R. Jacobson, R. M. Key, G. McKinley, J. L. Sarmiento, and R. Wanninkhof (2007), Constraining global air-sea gas exchange for CO₂ with recent bomb ¹⁴C measurements, *Global Biogeochem. Cycles*, 21, GB2015, doi:10.1029/2006GB002784.

1. Introduction

[2] A key element to understanding the cycling of soluble gases in the atmospheric and oceanic environments is parameterization of air-sea gas exchange. The standard approach, which uses wind speed to parameterize gas transfer velocity, has long been plagued by the fact that small-scale field experiments [Liss and Merlivat, 1986; Nightingale *et al.*, 2000] yield mean global gas transfer velocities (10–15.4 cm/hr) far smaller than estimates using global ocean inventories of either natural or bomb-produced radiocarbon (21.3–21.9 cm/hr, [Tans *et al.*, 1990; Wanninkhof, 1992]). In this study we have closed this gap between field and radiocarbon estimates by combining a much larger

database of dissolved inorganic radiocarbon, DI¹⁴C, measurements and a suite of ocean general circulation models in an inverse mode to interpolate the data in a manner consistent with ocean circulation.

[3] While small-scale field experiments have added significantly to our understanding of the factors that control gas transfer velocities over short time periods and specific regions of the world ocean, differences in fetch, surfactants, wind speed and mixed layer turbulence suggest an independent approach must be used to quantify air-sea gas exchange on a global scale. ¹⁴CO₂ is particularly useful for extrapolating gas exchange parameterizations to the global oceans for several reasons. First, it is an excellent analogue for gas exchange of CO₂ across the air-sea interface because it is nearly the same molecule. Second, the rate-limiting step for ocean bomb DI¹⁴C uptake is air-sea gas exchange and thus the radiocarbon budget is directly related to air-sea gas exchange. This is in contrast to CO₂ and other trace gases whose rate of uptake into the ocean is principally limited by exchange between the mixed layer and deeper layers of the ocean [Sarmiento *et al.*, 1992]. The air-sea gas exchange of ¹⁴CO₂ is rate limiting because the heavy isotope of carbon in CO₂ must completely exchange with the full inventory of CO₂, HCO₃⁻, and CO₃²⁻. This process takes roughly 10 times

¹Earth System Research Laboratory, NOAA, Boulder, Colorado, USA.

²Earth and Biosphere Institute, University of Leeds, Leeds, UK.

³Atmospheric and Ocean Sciences Program, Princeton University, Princeton, New Jersey, USA.

⁴Department of Atmospheric and Oceanic Sciences, University of Wisconsin-Madison, Madison, Wisconsin, USA.

⁵Atlantic Oceanographic and Meteorological Laboratory, NOAA, Miami, Florida, USA.

longer than the time needed to equilibrate the aqueous concentration of CO_2 [Broecker and Peng, 1982]. Third, the long equilibration time of $^{14}\text{CO}_2$ in the surface ocean provides an air-sea gas exchange signal needed to constrain the global long-term mean gas transfer velocity. Because the long-term mean incorporates the short-term spatial and temporal variability throughout the world oceans, $^{14}\text{CO}_2$ provides an important constraint for small-scale studies and a mechanism to scale these studies to levels relevant for modeling global trace gas budgets in the ocean.

[4] Over the last 50 years the air-sea partial pressure difference in $^{14}\text{CO}_2$ has changed by nearly an order of magnitude as a result of weapons testing in the 1960s. By balancing this large air-sea concentration gradient and the ocean bomb radiocarbon inventory ($\Delta\text{inv}(\text{Bomb DI}^{14}\text{C})$) over the last 50 years, a dimensionless constant γ can be estimated as

$$\gamma = \frac{\Delta\text{Inv}(\text{Bomb DI}^{14}\text{C})}{\int_{1954}^{1994} \int \frac{Sc(x, y, t)^{-0.5}}{660} u(x, y, t)_{10}^2 s(x, y, t) \Delta p^{14}\text{CO}_{2\text{bomb}}(x, y, t) dA dt}, \quad (1)$$

which provides a scaling factor for calculating the global mean gas transfer velocity, $k = \gamma(\text{Sc}/660)^{-1/2} u^2$ (Appendix A). Here s is solubility of aqueous CO_2 ($\text{mol m}^{-3} \text{atm}^{-1}$), u is the wind speed (m/s), $\Delta p^{14}\text{CO}_2$ is the partial pressure difference of bomb-produced $^{14}\text{CO}_2$ (atm) across the air-sea interface, dA is the area of the ocean being integrated, dt is the time period being integrated and Sc is the Schmidt number which takes into account deviations of the kinematic viscosity and the diffusion coefficient of CO_2 in seawater. Equation (1) is based on the approximations that natural radiocarbon is in a steady state and that a negligible fraction of the bomb-produced $^{14}\text{CO}_2$ ocean inventory has decayed in last 50 years.

[5] The bomb radiocarbon air-sea gas exchange constraint applied previously is biased for two reasons. First, the estimate of the ocean bomb radiocarbon inventory based on data from GEOSECS expeditions done in the 1970s [Broecker et al., 1985, 1995] is larger than estimates based on stratospheric bomb radiocarbon release and more recent estimates of the ocean bomb radiocarbon inventory using newer data sets [Hesshaimer et al., 1994; Joos, 1994; Key et al., 2004; Naegler and Levin, 2006; Peacock, 2004]. Second, the constraint if applied to air-sea gas exchange parameterizations has usually neglected spatio-temporal variation of air-sea concentration difference in $^{14}\text{CO}_2$. In total we find that these factors strongly bias both the total bomb $^{14}\text{CO}_2$ inventory and the air-sea concentration difference leading to a 33% decrease from previous estimates of the global gas transfer velocity for CO_2 calculated from equation (1).

2. An Improved Ocean Inventory of Bomb-Produced DI^{14}C

[6] Our reassessment of the ocean bomb-produced radiocarbon inventory is based on three methodological advances: (1) We have improved the methodology used to separate

bomb radiocarbon from natural radiocarbon; (2) we have combined data from expeditions done in the 1970s with those collected in the 1990s [Key et al., 2004] increasing the data density by almost an order of magnitude; and (3) we have used a suite ocean of GCMs to interpolate single point measurements made in time and space over the whole ocean from 1954 to 1998 in a method which is consistent with ocean transport.

[7] A significant part of this study addresses the biases associated with the separation of bomb-produced DI^{14}C from background DI^{14}C . The methodology used here is a modified version of the Rubin and Key [2002] approach which exploits the observation that background DI^{14}C throughout the world ocean has a pattern very similar to the one that emerges from the production and dissolution of CaCO_3 in the ocean. Using oxygen, alkalinity and nitrate measurements the natural background DI^{14}C can be pre-

dicted and subtracted from the contemporary measurements of DI^{14}C to estimate the concentration of bomb-produced DI^{14}C (Appendix B).

[8] Two other sources of potential bias are overcome with the much larger ocean radiocarbon data set from WOCE [Key et al., 2004] and better scheme for interpolating point measurements of DI^{14}C over space and time. The inclusion of almost 7500 more samples from WOCE expeditions in the 1990s avoids previous sampling biases due to scarcity of samples and location of samples taken [Peacock, 2004]. To interpolate the data in space and time in a manner consistent with ocean transport we make use of an inverse modeling technique similar to Gloor et al. [2003]. The approach uses model simulations to determine the specific ocean interior concentration patterns expected for a tracer (such as DI^{14}C) entering through 29 discrete surface regions of the ocean. The simulations thereby establish a linear relation

$$c_{\text{model}} = T f \quad (2)$$

between regional surface fluxes, f , and predicted ocean interior concentrations c_{model} . The i -th component of f is air-sea flux from region i in units of flux released for the forward simulations and the matrix T represents the effect of ocean transport and mixing on the tracers. Weighted linear least squares optimization [Lawson and Hanson, 1974] is used to find the fluxes f which minimize the difference between predicted and observed concentrations, $\|C_{\text{obs}} - C_{\text{mod}}\|$. Conversely, substituting c_{model} by the roughly 8000 observed bomb DI^{14}C values in equation (2) we can solve for surface fluxes,

$$f = T^{-1} c_{\text{obs}}. \quad (3)$$

[9] An important detail to this technique is that we use a simplifying assumption, verified in forward runs of OGCMs

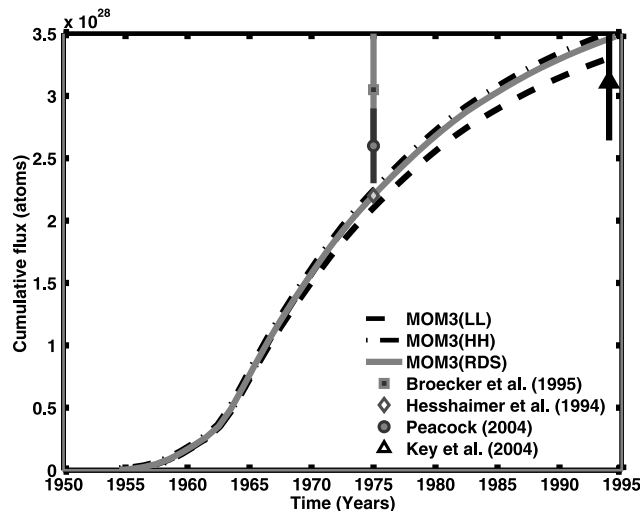


Figure 1. Estimated time history of bomb $^{14}\text{CO}_2$ inventory in the world oceans. Dashed, dash-dotted, and solid lines show cumulative inventory of $^{14}\text{CO}_2$ over the last 50 years using a suite of the GFDL MOM3 models to represent possible spread in time history of inventory due to model parameterizations of isopycnal velocity and diapycnal diffusion. The black square shows the Broecker *et al.* [1995] estimate, the open diamond circle shows the Hesshaimer *et al.* [1994] inventory estimate, the gray circle shows the Peacock [2004] estimate, and the open triangle is from GLODAP [Key *et al.*, 2004].

(Appendix C), that the flux into each of the 29 surface regions of the inversion has a time history proportional to the overlying atmospheric perturbation. A similar approach has been used for ocean inversions of anthropogenic CO_2 [i.e., Gloor *et al.*, 2003; Jacobson *et al.*, 2007a, 2007b]. Tracers are therefore injected with this prescribed time history. By prescribing a time history we only have to solve for one unknown per region as opposed to one unknown for every time interval for each region. As a result the number of unknowns is significantly reduced. The inventory of bomb-produced DI^{14}C from the air-sea flux estimates is given by

$$\Delta \text{Inv}(\text{Bomb } \text{DI}^{14}\text{C}) = \int_{1954}^{1994} \int_{\text{Ocean Surface}} f_{\text{Bomb } ^{14}\text{CO}_2} dA dt. \quad (4)$$

[10] Since deficiencies in modeled transport are a potential source of uncertainty, we base the inverse calculations on three versions of an OGCM with different subgrid-scale transport process parameterizations. Each model version has broadly realistic circulations and mixing characteristics according to mixed layer depths, ocean temperature and salinity distributions as well as rate of North Atlantic Deep Water formation [Gnanadesikan, 1999].

[11] The inventory estimates and their time evolution displayed in Figure 1 along with previous estimates reveal the following: (1) The total ocean inventory of bomb DI^{14}C

($343 \pm 40 \times 10^{26}$ atoms ^{14}C as of 1994) is only very weakly sensitive to transport representation (Figure 1); (2) our 1975 inventory is more than 25% below the estimates suggested by Broecker *et al.* [1985, 1995] which were later used to estimate the global gas transfer velocity [Tans *et al.*, 1990; Wanninkhof, 1992]; (3) the inventory for 1975 is in excellent agreement with estimates of Hesshaimer *et al.* [1994] based on stratospheric and tropospheric measurements of $^{14}\text{CO}_2$ and a three-box model; (4) the time history of the bomb-produced DI^{14}C inventory is consistent with Peacock [2004] and Key *et al.* [2004] given an error of 16% on the inventory trajectories. The poor agreement with Peacock [2004] may be due to the imposed flux history which could underestimate the total inventory in 1975 in order to meet the constraints of the data collected in the 1990s (Appendix C). Since the method in this study does take into account the area of the Arctic Ocean we expect our estimate to be higher than that estimated by Key *et al.* [2004] which does not take into account bomb-produced DI^{14}C in the Arctic Ocean.

3. A Gas Transfer Velocity Estimate From New Ocean Bomb $^{14}\text{CO}_2$ Inventory

[12] At first glance, a 25% decrease in the bomb-produced $^{14}\text{CO}_2$ inventory would suggest a 25% decrease in flux when air-sea gas exchange is tied to the revised ocean bomb radiocarbon inventory. However, in the original calculation based on equation (1), Wanninkhof [1992] assumed that the ocean surface had a uniform temperature of 20°C and a solubility of $33.3 \text{ mol m}^{-3} \text{ atm}^{-1}$ and that both atmosphere and ocean pCO_2 were $314 \times 10^{-6} \text{ atm}$.

[13] The Wanninkhof [1992] estimate has recently been updated by Naegler *et al.* [2006] using previous inventory estimates [Key *et al.*, 2004; Peacock, 2004] and the zonal mean history of DI^{14}C . While Naegler *et al.* [2006] did consider the spatial and temporal variability of winds, temperature, salinity and p^{12}CO_2 to compute γ for equation (1), they do not consider the zonal variations in surface DI^{14}C with time that occur as the result of ocean circulation. In contrast to previous approaches the inversion technique used here permits estimates of ocean surface DI^{14}C which are spatially, both in the zonal and meridional direction, and temporally resolved in a way that is consistent with ocean transport and the change in ocean inventory for bomb DI^{14}C over time. Using the estimates of DI^{14}C we can therefore resolve surface ocean p^{14}CO_2 temporally and spatially, enabling us to assess the biases that arise from assumptions made in previous studies. To convert DI^{14}C to p^{14}CO_2 three approximations were made (Appendix D): (1) changes in ocean surface temperature, salinity, nutrients and alkalinity are negligible in the annual mean over time; (2) ocean DIC and pCO_2 was adjusted over time to keep ΔpCO_2 constant; and (3) that the air-sea concentration difference of 1954 is entirely the result of the natural DI^{14}C distribution which is consistent with coral measurements and ocean measurements made in the 1950s [Rubin and Key, 2002].

[14] Accounting for spatial variation in solubility and air-sea difference in p^{14}CO_2 and the change in inventory the global gas transfer velocity is estimated to be $14.6 \pm 4.7 \text{ cm/hr}$, a substantial correction (33%) compared to the original calcu-

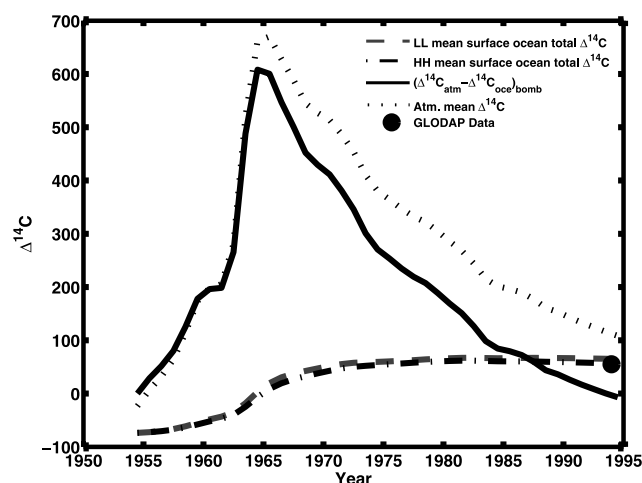


Figure 2. Atmospheric and ocean $\Delta^{14}\text{CO}_2$ (‰) from 1954 to 1994. Dotted (HH) and dashed (LL) lines show the area-weight mean $\Delta^{14}\text{CO}_2$ in the surface ocean using bomb-produced estimates from this study added to estimates of background $\Delta^{14}\text{CO}_2$ from Rubin and Key [2002]. The gray solid line is the calculated difference between bomb-produced atmospheric $\Delta^{14}\text{CO}_2$ and bomb-produced ocean $\Delta^{14}\text{CO}_2$. The black solid line shows the mean atmospheric $\Delta^{14}\text{CO}_2$ [Orr *et al.*, 2001]. The gray dot indicates the area-normalized mean $\Delta^{14}\text{CO}_2$ from the Global Ocean Data Analysis Project (GLODAP) [Key *et al.*, 2004]. The small difference in the surface estimates of $\Delta^{14}\text{CO}_2$ indicates that our estimate is not very sensitive to differences in modeled transport.

lation of 21.9 ± 3.3 cm/hr [Wanninkhof, 1992] and statistically equivalent to a more recent estimate of 16.7 ± 2.9 by Naegler *et al.* [2006]. Although most of the change in the estimated global gas transfer velocity from Wanninkhof [1992] is consistent with the change in inventory (25%), it turns out that assumptions of a constant solubility of $33.3 \text{ mol m}^{-3} \text{ atm}^{-1}$ calculated from the mean ocean temperature and salinity in the world ocean would account for another 6%. There is a 6% difference between the solubility calculated from the mean temperature and salinity of the world oceans and the mean solubility of the world ocean calculated on the MOM3 grid.

[15] Figure 2 shows that the difference in the mean surface ocean concentration of DI^{14}C between two very different MOM3 GCM runs is small compared to the air-sea difference in bomb-produced radiocarbon from 1954–1994. Because the transport models cannot reproduce the high temporal and spatial variability in the surface, we have decided not to include the estimates of bomb-produced DI^{14}C from the upper 30 m of the ocean in our inversion. This enabled us to independently evaluate this studies' estimate of p^{14}CO_2 at the surface with that calculated from the Global Ocean Data Analysis Project (GLODAP, gray dot) for 1994. Agreement between our estimates and the independent data supports this studies' estimate of surface ocean p^{14}CO_2 through time given that our estimates are so heavily constrained by deep water measurements and not near surface measurements, even those just below 30 m.

[16] Our approach is a significant improvement over previous studies because it combines a larger database of ocean measurements with a spatio-temporal interpolation technique consistent with modeled ocean circulation. Despite these improvements, it is important to consider the magnitude of our uncertainties in equation (1). For the inventory estimate two sources of errors need to be considered. The first is the uncertainty of the estimated bomb-produced DI^{14}C in ocean which can be derived from our ability to estimate the natural DI^{14}C ($\pm 15\%$ [Key *et al.*, 2004]). The second is the uncertainty derived from the inversion ($\pm 7\%$). For the inversion, the formal error estimate is small because there are so many ocean measurements (~ 8000) relative to parameters being determined (29). Most of the error for the inversion comes from the uncertainty in modeled transport that is not captured by formal error propagation. For the denominator in equation (1), the most significant source of error is in the estimate of $\Delta \text{p}^{14}\text{CO}_2$. While large differences are observed regionally in the surface ocean for different MOM3 GCM runs, little difference is seen between the global means for p^{14}CO_2 (Figure 2). Thus we estimate an uncertainty of 15%.

[17] Combining all the possible errors gives a total of 4.7 cm hr^{-1} for the global gas transfer velocity which makes this estimate ($14.6 \pm 4.7 \text{ cm hr}^{-1}$) significantly less than the original estimates ($21.9 \pm 3.3 \text{ cm hr}^{-1}$ [Wanninkhof, 1992]). While the uncertainty that we calculate includes a contribution due to uncertainty in model circulations, our estimated value is based on the data fit to the transport model with low vertical diffusivity and horizontal mixing (LL). We have chosen this simulation because the independent forward runs of CFC-11 with this model version in this transport matrix most closely match observations [Gnanadesikan *et al.*, 2002].

4. Implications for a New Global Gas Transfer Velocity

[18] A necessary criterion for any valid gas exchange parameterization for the global oceans is consistency with the bomb radiocarbon budget. In the past, this criterion has been met by effectively increasing the gas transfer velocity measured in the field by $\sim 25\%$ to agree with the DI^{14}C inventory. The agreement between the global average gas transfer velocity derived from this study and the study of Nightingale *et al.* [2000], which is based on short-term (3–20 days) field experiments, removes this requirement. The agreement is illustrated in Figure 3.

[19] Figure 3 shows the Wanninkhof [1992] short-term wind formulation using the quadratic dependence of the gas transfer velocity on wind speed for an open ocean (no ice) global mean wind speed at 10 m, $u_{10} = 6.89 \text{ m s}^{-1}$ and variance estimated from the NCEP/NCAR Reanalysis 1 1954–2000 [Kalnay *et al.*, 1996]. It should be noted that the original formulation used by Wanninkhof [1992] assumed that $u_{10} = 7.4 \text{ m s}^{-1}$ was an average global wind speed and that a Rayleigh distribution best described how short-term winds were distributed about the mean. A comparable curve has been computed on the basis of the global bomb DI^{14}C inventory from this study using equation (1) and Appendix A. As with the global mean gas exchange velocities the wind

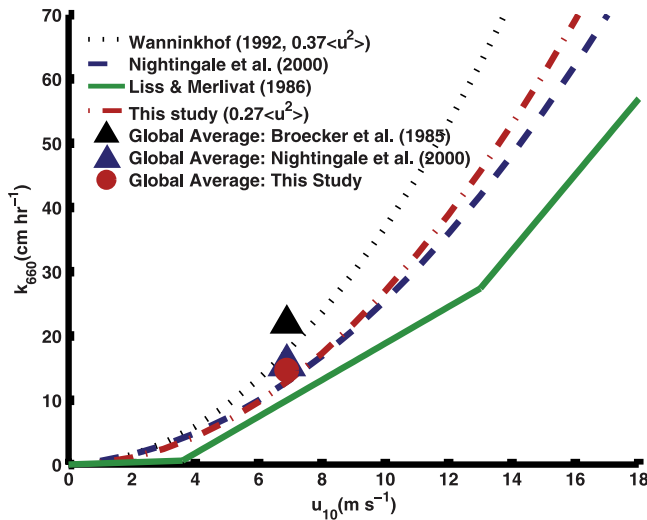


Figure 3. Gas transfer velocity (cm hr^{-1}) as a function of wind speed (m s^{-1}). Black dotted line shows short-term wind (steady wind) relationship of Wanninkhof [1992] corrected for the mean of the ocean NCEP/NCAR Reanalysis 1 1954–2000 wind speed squared ($\langle u^2 \rangle$) [Kalnay et al., 1996]. Red dash-dotted line shows the short-term wind ($\langle u^2 \rangle$) relationship developed from ^{14}C inventory in this study assuming a quadratic relationship between wind and gas transfer velocity. Blue triangles solid blue and gray lines show Nightingale et al. [2000] and Liss and Merlivat [1986] short-term wind relationships, respectively.

speed versus gas transfer velocity relationships for this study and Wanninkhof [1992] are very different.

5. Impact on Global Air-Sea Gas Exchange Estimates

[20] To put the parameterizations of gas transfer velocity into context with other estimates of carbon uptake in the

world ocean the air-sea gas flux has been computed by estimating the exchange of CO_2 ($\text{mol C m}^{-2} \text{ yr}^{-1}$),

$$F_{\text{CO}_2} = \int_{1995}^{1995} \int_{\text{Surface Ocean}} k_s \Delta p \text{CO}_2 dA dt. \quad (5)$$

[21] From the $\Delta p \text{CO}_2$ climatology [Takahashi et al., 2002] and the NCEP/NCAR Reanalysis 1 1954–2000 wind speeds, the net air-sea gas exchange calculated from this study is $1.3 \pm 0.5 \text{ Pg C yr}^{-1}$ (assuming 25% error in the $\Delta p \text{CO}_2$ [Takahashi et al., 2002]) for 1995. Adding an extra $0.45 \pm 0.2 \text{ Pg C yr}^{-1}$ to account for the carbon that enters the ocean through rivers every year [Jacobson et al., 2007a, 2007b], the net ocean uptake would be $1.8 \pm 0.5 \text{ Pg C yr}^{-1}$. A comparison of air-sea CO_2 flux estimates using four different methods indicates that our estimate is consistent with other independent estimates (Table 1). From a methodological point of view ocean interior data-based methods and estimates based on the oxygen to nitrogen ratio are likely to give the most robust estimates over decadal time-scales because they take advantage of the fact that ocean interior tracer concentrations and the atmospheric O_2/N_2 ratios are the result of long-term average fluxes of CO_2 into the ocean. Several recent studies have demonstrated the accuracy of the inverse method using interior ocean measurements through careful analysis which has reduced uncertainties in these estimates to $\pm 0.25 \text{ PgC yr}^{-1}$ [Jacobson et al., 2007a, 2007b; Matsumoto and Gruber, 2005].

[22] While the agreement between different methods for the net global air-sea gas exchange is gratifying, it is important to understand the limitations in using air-sea gradient to calculate a net air-sea gas exchange. Both the estimate of $\Delta p \text{CO}_2$ and wind are large sources of bias. Although the $\Delta p \text{CO}_2$ climatology [Takahashi et al., 2002] includes more than 1.8 million measurements, the distribution of measurements in the Southern temperate and sub-polar regions of the world oceans is sparse in space as well

Table 1. Compilation of Net Annual Oceanic Uptake of CO_2 Estimates for 1990s^a

Study	Description	Global Ocean Flux, PgC yr^{-1}
This study	$k_s = 0.27 \langle u_{10}^2 \rangle (Sc/660)^{-0.5}$	1.8 ± 0.5
Sabine et al. [2004]	based on difference in DIC measurements and estimates of DIC concentrations before industrial revolution with correction for river flux (1980–1998)	2.4 ± 0.5
Gurney et al. [2003]	inversion estimate based on multiple atmospheric transport models and observed atmospheric CO_2 (1992–1996)	2.0 ± 1.3
McNeil et al. [2003]	ages estimated from observed CFC (1980–1999)	2.0 ± 0.4
Gloor et al. [2003]	Inversions based on ocean transport models and observed ocean DIC (1990)	1.8 ± 0.4
Mikaloff Fletcher et al. [2006]	inversion based on multiple ocean transport models and observed ocean DIC (1995)	2.2 ± 0.3
Matsumoto et al. [2004]	forward model simulations evaluated with CFCs and pre-bomb radiocarbon (1990s)	2.2 ± 0.2
Bopp et al. [2002]	based on measured atmospheric O_2/N_2 and CO_2 concentrations corrected for ocean warming and stratification using forward model calculations (1990–1996)	2.3 ± 0.7
Jacobson et al. [2007a, 2007b]	joint inversion based on atmospheric and oceanic observations and models (1995)	2.2 ± 0.3

^aIn this study, oceanic uptake was calculated using winds from the NCEP/NCAR Reanalysis 1 1954–2000 [Kalnay et al., 1996] and the Takahashi et al. [2002] surface ocean $p\text{CO}_2$ climatology assuming an annual $0.45 \pm 0.2 \text{ PgCyr}^{-1}$ flux of DIC from rivers [Jacobson et al., 2007a, 2007b]. All other calculations shown here for net annual oceanic uptake (with the exception of Matsumoto et al. [2004]) do not depend on the gas exchange parameterization.

as time. The coastal regions, where $\Delta p\text{CO}_2$ variability is high and difficult to predict, are also undersampled. In addition to the $\Delta p\text{CO}_2$ climatology, global estimates of wind speed show significant variability between products in the magnitude of spatial variability and regional and global means. The result is that although our bomb DI^{14}C constraint on gas exchange should be independent of wind speed product there will be some variability in the global net gas exchange due to differences in regional variability of wind speed between wind reanalysis products. Since γ uniquely depends on the first two moments of the wind product used, no single γ can be applied for all wind products.

6. Conclusion

[23] Using a suite of ocean models in the inverse mode and a newly available database of DI^{14}C measurements an estimate of the world ocean inventory of bomb-produced DI^{14}C during the period from 1954 to 1998 was produced. These ocean inventory estimates are in agreement with estimates based on stratospheric and tropospheric measurements of $^{14}\text{CO}_2$ and suggest that previous estimates of Broecker *et al.* [1985, 1995] are high by 25%. Constraining the mean global gas transfer velocity of CO_2 with the ocean inventory of bomb-produced DI^{14}C and inversion-produced estimates of $p^{14}\text{CO}_2$ leads to 33% decrease from previous estimates. This adjustment in the global mean gas transfer velocity of CO_2 finally closes the gap between global-scale radiocarbon-based estimates and small-scale dual tracer studies, which now agree.

[24] This study provides an important constraint for modeling air-sea gas exchange on global scales as well as local scales. This study also suggests that while the net annual ocean uptake of CO_2 calculated from climatological estimates of surface $\Delta p\text{CO}_2$ and wind speed agree with other independent estimates there are many sources of bias in this estimate that must be considered.

Appendix A: Derivation of the Global Average Transfer Velocity

[25] This study exploits the fact that the highest resistance (and the largest gradient) of aqueous $^{14}\text{CO}_2$ is across the air-sea interface. The net gas exchange can be expressed as $F = k_s(p_a - p_w)$ where the gas transfer velocity, $k = D/h$, h is thickness of the air-sea interface, D is diffusivity ($\text{m}^2 \text{s}^{-1}$), s is the solubility and p_a is the partial pressure of a gas in the surface waters at equilibrium with the atmospheric boundary layer and p_w is the measured partial pressure of the gas in the water. To account for the nonideality of the gas transfer velocity model due to changes in temperature, salinity, gas and turbulence the gas transfer velocity is often parameterized as $k = \gamma(\text{Sc})^n f(u_{10})$ where Sc is the Schmidt number (ν/D , ν is the kinematic viscosity), γ and n are dimensionless constants and $f(u_{10})$ is an analogue for frictional velocity (distance/time). The Schmidt number accounts for differences in the rates at which individual gases pass across the air-sea interface at a given temperature and salinity. For this study we have followed the logic of Wanninkhof [1992] which suggests that gas exchange is a quadratic function of wind speed as suggested by many

short-term field experiments [Nightingale *et al.*, 2000; Wanninkhof *et al.*, 1985] and that $n = -1/2$. Using the formulation for the net air-sea gas exchange, the total flux $^{14}\text{CO}_2$ across the air-sea interface is

$$F_{\text{co2}}^{14} = \iiint \gamma \frac{\text{Sc}(x,y,t)^{-0.5}}{660} u(x,y,t)^2 s(x,y,t) \Delta^{14}\text{CO}_2(x,y,t) dx dy dt. \quad (\text{A1})$$

[26] Because the decay of bomb-produced $^{14}\text{CO}_2$ is considered to be negligible over 50 years, the total flux of bomb-produced $^{14}\text{CO}_2$ into the ocean should be equal to the change in inventory of bomb-produced $^{14}\text{CO}_2$ in the ocean ($\Delta \text{Inv}(\text{Bomb } \text{DI}^{14}\text{C})$). Thus we can calculate the scalar γ accounting for the all the covariance terms in spatial and temporal variability of wind speed, solubility and Schmidt number as

$$\gamma = \frac{\Delta \text{Inv}(\text{Bomb } \text{DI}^{14}\text{C})}{\iiint \frac{\text{Sc}(x,y,t)^{-0.5}}{660} u(x,y,t)^2 s(x,y,t) \Delta p^{14}\text{CO}_{2\text{bomb}}(x,y,t) dx dy dt}. \quad (\text{A2})$$

[27] To calculate γ for short-term winds we use the mean of u_{10}^2 calculated from the NCEP/NCAR Reanalysis 1 1954–2000 [Kalnay *et al.*, 1996] of 6 hour winds. An analysis of how our result would change using monthly means in solubility and Schmidt numbers shows that there is little effect. This is partly due to the fact that our inversion only calculates annual means for $\Delta p^{14}\text{CO}_{2\text{bomb}}$ across our model grid. For this reason our calculation at a monthly resolution will only be affected by the covariance between solubility, Schmidt numbers and winds.

[28] It is important to stress that the value of γ uniquely depends on the temporal and spatial resolution of u_{10}^2 [Naegler *et al.*, 2006]. This is illustrated by comparing the γ using the mean u_{10}^2 ($\gamma = 0.27$) and the mean u_{10} ($\gamma = 0.31$) of the NCEP/NCAR Reanalysis 1 1954–2000 mapped on to a 6 hour and $3.75^\circ \times 4.5^\circ$ grid. The large difference in γ implies that γ uniquely depends on the first two moments of the wind product used and that no single γ can be applied for all wind products.

Appendix B: Estimating the Inventory of Bomb-Produced $^{14}\text{CO}_2$ in the World Oceans

[29] Over the last 20 years there has been an ongoing debate concerning the size of the bomb DI^{14}C inventory that has entered the ocean since the onset of weapons testing in the late fifties. In two separate studies, Broecker *et al.* [1985] estimated that a little over 3.05×10^{28} atoms of ^{14}C had entered the ocean by the time the GEOSECS measurements of DI^{14}C were done (~ 1975). Hesshaimer *et al.* [1994] challenged Broecker's estimate with an ocean-land-atmospheric box model which was calibrated against atmospheric measurements of $^{14}\text{CO}_2$ and determined that only about 2.25×10^{28} atoms of ^{14}C could have entered the ocean by 1975 if stratospheric inventories were correct. Since then several studies have indicated that Broecker's ocean inventory estimate was too high. In particular, Peacock

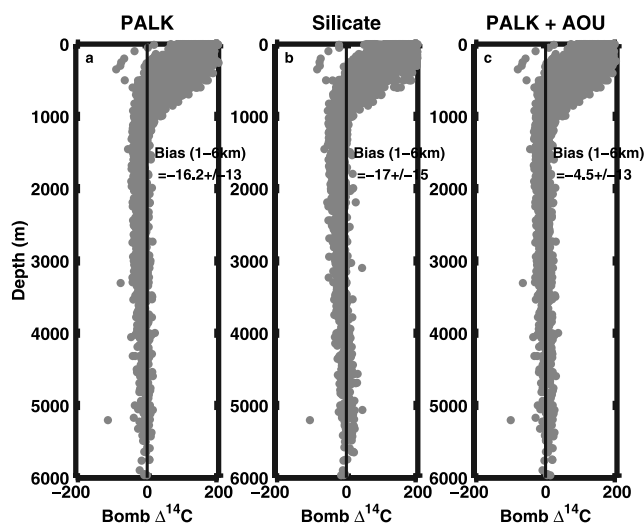


Figure B1. Estimated bomb-produced $\Delta^{14}\text{CO}_2$ (‰) profiles in Pacific Ocean. (a) Estimates of bomb-produced $\Delta^{14}\text{CO}_2$ from Rubin and Key [2002]. (b) Estimates of bomb-produced $\Delta^{14}\text{CO}_2$ from Broecker et al. [1995]. (c) Estimates of bomb-produced $\Delta^{14}\text{CO}_2$ using both potential alkalinity (PALK) and apparent oxygen utilization (AOU) fit to deep water measured $\Delta^{14}\text{CO}_2$ values where CFC-11 was below 0.1 parts per trillion.

[2004] pointed out that the locations of GEOSECS stations may have biased the inventory estimate by as much as 25% too high. In a separate study, Key et al. [2004] used more recent World Ocean Circulation Experiment (WOCE) measurements to estimate that 3.13×10^{28} atoms of ^{14}C had entered the ocean by 1995. Following Broecker et al. [1995] the ocean bomb DI^{14}C inventory should have increased by another 25% from 1975–1995 making the Key et al. [2004] inventory consistent with Hesshaimer et al.'s [1994] estimate. Using an inverse technique to interpolate point estimates of bomb DI^{14}C in space and time we confirm that the original bomb DI^{14}C inventory estimates made by Broecker et al. [1985, 1995] were indeed 25% too high given the time the measurements were made (Figure 1).

[30] An important component in estimating the bomb DI^{14}C inventory has been the method by which the bomb ^{14}C is separated from the natural concentration of DI^{14}C that existed before weapons testing was started. The first two separation methods were introduced by Broecker et al. [1985, 1995] using tritium and silicate. In the case of tritium (^3H) it was assumed that all the tritium was bomb produced and penetrated the ocean on the same timescale and physical pathways as bomb-produced $^{14}\text{CO}_2$, allowing “bomb” DI^{14}C to be subtracted from the total DI^{14}C measured in the ocean. While bomb-produced tritium and $^{14}\text{CO}_2$ were released into the atmosphere in the same way, tritium is scavenged from the atmosphere via precipitation whereas $^{14}\text{CO}_2$ enters the oceans via gas exchange. As an alternative to the tritium method, Broecker et al. [1995] utilized an empirical relationship between deep water silicate and DI^{14}C to predict the natural background ocean DI^{14}C . Although high silicate concentrations are matched by low DI^{14}C values throughout the deep ocean, the relationship in the Southern Ocean (South of

$\sim 50^\circ\text{S}$) is quite different from the rest of the deep ocean. Thus, using silicate concentrations creates a discontinuity in the estimated natural background ocean DI^{14}C wherever a Southern Ocean boundary is assumed to be.

[31] Seeking a tighter relationship that could be applied to all of the world oceans a third approach was developed by Rubin and Key [2002]. This approach utilizes the fact that the change in alkalinity of the ocean due to the dissolution and precipitation of CaCO_3 is coincident with the relative age of water masses and thus the natural background DI^{14}C . Since alkalinity in the ocean is also affected by the remineralization and production of organic carbon through the addition and subtraction of NO_3^- , respectively, a correction must be made to the alkalinity measurements. This can be done by adding the nitrate concentration to the alkalinity which produces a quantity called potential alkalinity (PALK) where

$$\text{PALK} = (\text{Alkalinity} + \text{nitrate}) * 35 / \text{salinity}. \quad (\text{B1})$$

The salinity normalizes the effect of freshwater on alkalinity.

[32] Although the relationship between PALK and natural DI^{14}C is very tight throughout the deep Pacific ocean, profiles of the bomb-produced DI^{14}C result in negative mean values from 1000 m to the bottom where the average values should be zero (Figure B1a) suggesting a negative bias in the potential alkalinity based method. To correct for this apparent bias, oxygen was used in addition to PALK to estimate background (or natural) DI^{14}C . By regressing waters containing less than 0.1 ppt Chlorofluorocarbon-11

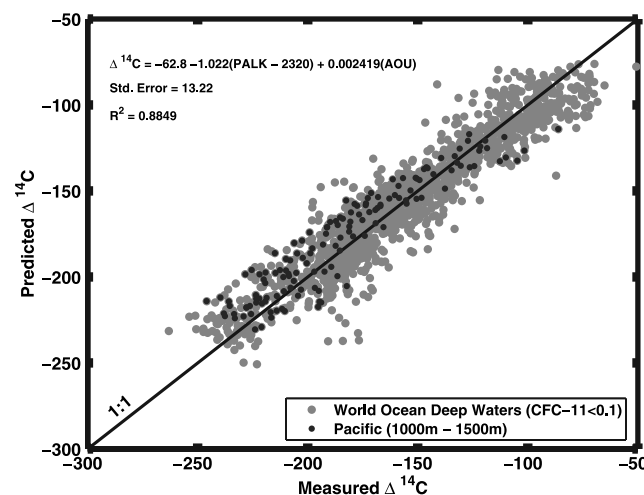


Figure B2. Multiparameter fit of measured $\Delta^{14}\text{CO}_2$ (‰) versus predicted $\Delta^{14}\text{CO}_2$ using both potential alkalinity (PALK) and apparent oxygen utilization (AOU). The fit (Natural $\Delta^{14}\text{C} = -62.80 - 1.022(\text{PALK} - 2320) + 0.0024(\text{AOU})$, $n = 1577$, $R^2 = 0.88$ and standard error = 13‰) shows that data collected from the Pacific between 1500 and 2000 (black dots) are slightly overestimated compared to the measurements. However, this is an improvement over existing estimates of natural $\Delta^{14}\text{CO}_2$ in Pacific sector of the world oceans (gray dots).

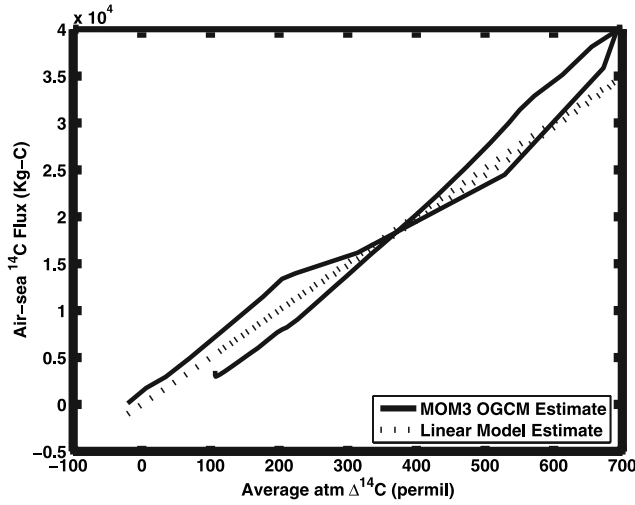


Figure C1. Linear response of annual air-sea flux of $^{14}\text{CO}_2$ to atmospheric concentration 1954–1999. The thick black line represents the global total flux of $^{14}\text{CO}_2$ in an OCMIP2 (Ocean Carbon-cycle Model Intercomparison Project) [Orr *et al.*, 2001] forward run and is plotted against the history of the atmospheric perturbation assumed in that simulation. A simple linear model of regional flux (equation (C1)) as a function of local atmospheric concentration was constructed for each of 29 discrete ocean regions. The sum of the regional predictions is represented by the dotted black line. The differing atmospheric history of $^{14}\text{CO}_2$ as a function of latitude in the OCMIP2 simulation is responsible for the nonlinearity of the prediction.

(CFC-11) to PALK and Apparent Oxygen Utilization (AOU) (Figure B2) we derived the following in which

$$\text{AOU} = \text{O}_{2\text{sat}} - \text{O}_{2\text{meas}}, \quad (\text{B2})$$

$$\text{Natural } \Delta^{14}\text{C} = -62.80 - 1.022(\text{PALK} - 2320) + 0.0024 \times (\text{AOU}), \quad (\text{B3})$$

$$\text{DI}^{14}\text{C} = \text{DI}^{12}\text{C} \cdot 1.176 \cdot 10^{-12} \left(1 + \text{Natural } \Delta^{14}\text{C} / 1000 \right), \quad (\text{B4})$$

where $\text{O}_{2\text{meas}}$ and $\text{O}_{2\text{sat}}$ are the measured and saturated oxygen concentrations at in situ potential temperatures. By adding AOU to the regression the bias using the potential alkalinity and silicate methods is well within the standard deviation of deep water bomb-produced DI^{14}C estimates (Figure B1). Because AOU is nearly always zero at the surface this correction has little effect on the estimated values of the natural DI^{14}C in surface waters. For regions of the ocean where AOUs are smaller, such as the Indian and Atlantic Oceans the correction to the natural DI^{14}C are much smaller. Correcting for the midwater bias in the Pacific by using AOU to predict the natural DI^{14}C increases the estimates of bomb-produced DI^{14}C by $\sim 5\%$. While the addition of AOU does remove the bias below 1000 m in the Pacific it does not improve standard error of the

predicted background DI^{14}C using the approach of Rubin and Key [2002] (Figure B2).

Appendix C: Linear Relationship Between Atmospheric History and Flux as Exhibited by Forward Model Simulations

[33] An important detail in our inverse analysis of bomb DI^{14}C is that we assume that the flux into a given region has a time history very similar to the overlying atmospheric perturbation. This assumption provides us with two advantages: (1) We can dramatically reduce the number of variables we are solving for [Gloor *et al.*, 2003; Jacobson *et al.*, 2007a, 2007b] and (2) we can interpolate over a sparse set of measurements with respect to time.

[34] To justify this assumption we compared air-sea flux in a forward OGCM simulation of DI^{14}C from 1954 to 1999 to a linear statistical model where the flux into each region is exactly proportional to atmospheric history through time (Figure C1) such that

$$F_{\text{co2}}^{14}(t) \propto p^{14}\text{CO}_{2\text{atm}}(t) - p^{14}\text{CO}_{2\text{atm}}(1954). \quad (\text{C1})$$

[35] While there is not a perfect match between the simple linear model and forward OGCM simulation in Figure C1, within the errors of the forward OGCM simulation it is a good first-order assumption. Close inspection shows that the yearly flux in the forward OGCM simulation was up to 12% higher during times when the atmospheric $^{14}\text{CO}_2$ was at its peak suggesting that the ocean surface $p^{14}\text{CO}_2$ is lagged behind the spike in atmospheric $^{14}\text{CO}_2$ in the forward model making the annual flux estimate more responsive than the simple linear model. In total, this implies that the linear assumption made in the inversion tends to underestimate the flux of bomb-produced DI^{14}C into the ocean before 1975 and overestimate the flux bomb-produced DI^{14}C into the ocean after 1975. Because the majority of the data (more than 90%) of the data is from the 1990s the least squares technique we are using for the inversion will tend to weigh the fit to the data collected in 1990s. Although this will not bias either the inventory as of 1994 or scaling factor for the mean global gas transfer velocity (equation (1)) it suggests that the 1975 inventory may be biased low by as much as 10%.

Appendix D: Calculation of the Air-Sea $^{14}\text{CO}_2$ Gradient in the Surface Oceans Between 1954 and 1994

[36] A final component to the gas transfer velocity estimate is the calculation of an air-sea gradient in aqueous $^{14}\text{CO}_2$ concentration, $s\Delta p^{14}\text{CO}_2$, accounting for kinetic and species fractionation of dissolved inorganic carbon ($\text{DIC} = [\text{CO}_2] + [\text{CO}_3^{2-}] + [\text{HCO}_3^-]$) we define a concentration gradient over the stagnant layer as

$$s\Delta p^{14}\text{CO}_2 = \alpha_k \alpha_{\text{aq-g}} s \left(\left(\frac{\text{DI}^{14}\text{C}_{\text{atm}}}{\text{DI}^{12}\text{C}_{\text{atm}}} \right) p\text{CO}_{2\text{atm}} - \left(\frac{\text{DI}^{14}\text{C}_{\text{oce}}}{\text{DI}^{12}\text{C}_{\text{oce}} \alpha_{\text{DIC-g}}} \right) p\text{CO}_{2\text{oce}} \right), \quad (\text{D1})$$

where α_k , $\alpha_{\text{aq-g}}$, $\alpha_{\text{DIC-g}}$ are the kinetic and aqueous to gas and DIC to gas isotope fractionation corrections for $^{14}\text{CO}_2$ from Zhang *et al.* [1995] accounting for doubling in fractionation between $^{13}\text{CO}_2/^{12}\text{CO}_2$ and $^{14}\text{CO}_2/^{12}\text{CO}_2$. The $p\text{CO}_{2\text{oce}}$ and $p\text{CO}_{2\text{atm}}$ are the partial pressure of CO_2 in the ocean and atmosphere, respectively. The DI^{12}C and DI^{14}C are the total CO_2 (including HCO_3^- and CO_3^{2-}) for the respective isotopes.

[37] While $p\text{CO}_{2\text{atm}}$, $\text{DI}^{12}\text{C}_{\text{atm}}$ and $\text{DI}^{14}\text{C}_{\text{atm}}$ can be estimated directly from atmospheric records [GLOBALVIEW, 2005], estimation of $p\text{CO}_{2\text{oce}}$, $\text{DI}^{12}\text{C}_{\text{oce}}$ and $\text{DI}^{14}\text{C}_{\text{oce}}$ requires some approximations. To estimate $p\text{CO}_{2\text{oce}}$, and $\text{DI}^{12}\text{C}_{\text{oce}}$ it was assumed that the surface water alkalinity stayed constant within the grid domain of the MOM3 OGCM from 1954–1994. Because the MOM3 and GLODAP grids do not fully overlap GLODAP alkalinity has been extrapolated to the MOM3 grid using the approach introduced by Millero *et al.* [1998]. In this approach surface temperature (SST) and salinity (S) are used to estimate surface alkalinity throughout the ocean surface. The resulting fit to the total alkalinity (TALK),

$$\text{TALK} = -1.8017(\text{SST}) + 56.214(\text{S}) + 381.4, \quad (\text{D2})$$

gives a good estimate of alkalinity ($r^2 = 0.94$, $n = 7901$, Std. Err = 13.86 ($\mu\text{mol/Kg}$)) throughout the world oceans using the SST and salinity from the World Ocean Atlas [Conkright *et al.*, 2002].

[38] It was also assumed that the $\Delta p\text{CO}_2$ stayed constant from 1954–1994. Using a constant alkalinity and $\Delta p\text{CO}_2$, the temporal trend in the surface $p\text{CO}_{2\text{oce}}$ and $\text{DI}^{12}\text{C}_{\text{oce}}$ was calculated [Peng *et al.*, 1987] using the temporal trend in atmospheric $p\text{CO}_2$ data derived from GLOBALVIEW [2005] and the 1995 surface $p\text{CO}_2$ from Takahashi *et al.* [2002]. Because there are no estimates for $p\text{CO}_{2\text{oce}}$ in the Mediterranean Sea in the Takahashi *et al.* [2002] climatology, it was assumed that it was 360 ppm in 1995.

[39] Additionally, this analysis showed that the ice mask was an important component of the spatially integrated $s(\Delta p^{14}\text{CO}_2)$ calculation. An annual ice mask was constructed using a monthly ice mask from the Ocean Circulation Model Intercomparison Project (OCMIP) [Orr *et al.*, 2001]. For each grid point in the MOM3 ocean model the average annual ice coverage was calculated (X_{ice}). Assuming that the flux of $^{14}\text{CO}_2$ across the air-sea interface is linearly dependent on $(1 - X_{\text{ice}})$, the area-weighted integral of $s(\Delta p^{14}\text{CO}_2)$ was corrected for ice cover.

[40] **Acknowledgments.** This work was supported by an award from the National Science Foundation to Princeton University as well as the Geophysical Fluids Dynamics Lab which is a part of the National Oceanic and Atmospheric Administration, U.S. Department of Commerce. The data analyzed in this study is the result of a collaborative effort (GLODAP) by hundreds of scientists to put together data from many cruises connected with the GEOSECS, WOCE and JGOFS programs. The NCAR/NCEP Reanalysis 1 data was provided by the NOAA/OAR/ESRL PSD, Boulder, Colorado, from their Web site at <http://www.cdc.noaa.gov/>. Special thanks also go to Corinne Le Quéré and two anonymous reviewers for their comments and suggestions.

References

- Bopp, L., C. Le Quéré, M. Heimann, A. C. Manning, and P. Monfray (2002), Climate-induced oceanic oxygen fluxes: Implications for the contemporary carbon budget, *Global Biogeochem. Cycles*, 16(2), 1022, doi:10.1029/2001GB001445.
- Broecker, W. S., and T. H. Peng (1982), *Tracers in the Sea*, 689 pp., Columbia Univ. Press, New York.
- Broecker, W. S., T. H. Peng, G. Ostlund, and M. Stuiver (1985), The distribution of bomb radiocarbon in the ocean, *J. Geophys. Res.*, 90, 6953–6970.
- Broecker, W. S., S. Sutherland, W. Smethie, T. H. Peng, and G. Ostlund (1995), Oceanic radiocarbon—Separation of the natural and bomb components, *Global Biogeochem. Cycles*, 9, 263–288.
- Conkright, M. E., R. A. Locarnini, H. E. Garcia, T. D. O'Brien, T. P. Boyer, C. Stephens, and J. I. Antonov (2002), World Ocean Atlas 2001: Objective analyses, data statistics, and figures, CD-ROM documentation, *Internal Rep. 17*, 17 pp., Natl. Oceanogr. Data Cent., Silver Spring, Md.
- GLOBALVIEW (2005), *GLOBALVIEW-CO₂: Cooperative Atmospheric Data Integration Project—Carbon Dioxide* [CD-ROM], Natl. Oceanogr. Atmos. Admin. Clim. Monitoring and Diagnostics Lab., Boulder, Colo. [Also available on Internet via anonymous FTP to <ftp.cmdl.noaa.gov>, Path: [cg/co2/GLOBALVIEW](ftp://ftp.cmdl.noaa.gov/cg/co2/GLOBALVIEW)]
- Gloor, M., N. Gruber, J. Sarmiento, C. L. Sabine, R. A. Feely, and C. Rodenbeck (2003), A first estimate of present and preindustrial air-sea CO_2 flux patterns based on ocean interior carbon measurements and models, *Geophys. Res. Lett.*, 30(1), 1010, doi:10.1029/2002GL015594.
- Gnanadesikan, A. (1999), A simple predictive model for the structure of the oceanic pycnocline, *Science*, 283, 2077–2079.
- Gnanadesikan, A., R. D. Slater, N. Gruber, and J. L. Sarmiento (2002), Oceanic vertical exchange and new production: A comparison between models and observations, *Deep Sea Res., Part II*, 49(1–3), 363–401.
- Gurney, K. R., et al. (2003), TransCom 3 CO_2 inversion intercomparison: 1. Annual mean control results and sensitivity to transport and prior flux information, *Tellus, Ser. B*, 55, 555–579.
- Hesshaimer, V., M. Heimann, and I. Levin (1994), Radiocarbon evidence for a smaller oceanic carbon-dioxide sink than previously believed, *Nature*, 370, 201–203.
- Jacobson, A. R., S. E. Mikaloff Fletcher, N. Gruber, J. L. Sarmiento, and M. Gloor (2007a), A joint atmosphere-ocean inversion for surface fluxes of carbon dioxide: 1. Methods and global-scale fluxes, *Global Biogeochem. Cycles*, 21, GB1019, doi:10.1029/2005GB002556.
- Jacobson, A. R., S. E. Mikaloff Fletcher, N. Gruber, J. L. Sarmiento, and M. Gloor (2007b), A joint atmosphere-ocean inversion for surface fluxes of carbon dioxide: 2. Regional results, *Global Biogeochem. Cycles*, 21, GB1020, doi:10.1029/2006GB002703.
- Joos, F. (1994), Bomb radiocarbon—Imbalance in the budget, *Nature*, 370, 181–182.
- Kalnay, E., et al. (1996), The NCEP/NCAR 40-year reanalysis project, *Bull. Am. Meteorol. Soc.*, 77, 437–471.
- Key, R. M., A. Kozyr, C. L. Sabine, K. Lee, R. Wanninkhof, J. L. Bullister, R. A. Feely, F. J. Millero, C. Mordy, and T. H. Peng (2004), A global ocean carbon climatology: Results from Global Data Analysis Project (GLODAP), *Global Biogeochem. Cycles*, 18, GB4031, doi:10.1029/2004GB002247.
- Lawson, C. L., and R. J. Hanson (1974), *Solving Least Squares Problems*, Prentice-Hall, Upper Saddle River, N. J.
- Liss, P. S., and L. Merlivat (1986), Air-sea gas exchange rates: Introduction and synthesis, in *The Role of Air-Sea Exchange in Geochemical Cycling*, edited by P. Buat-Menard, pp. 113–127, Springer, New York.
- Matsumoto, K., and N. Gruber (2005), How accurate is the estimation of anthropogenic carbon in the ocean? An evaluation of the Delta C* method, *Global Biogeochem. Cycles*, 19, GB3014, doi:10.1029/2004GB002397.
- Matsumoto, K., et al. (2004), Evaluation of ocean carbon cycle models with data-based metrics, *Geophys. Res. Lett.*, 31, L07303, doi:10.1029/2003GL018970.
- McNeil, B. I., R. J. Matear, R. M. Key, J. L. Bullister, and J. L. Sarmiento (2003), Anthropogenic CO_2 uptake by the ocean based on the global chlorofluorocarbon data set, *Science*, 299, 235–239.
- Mikaloff Fletcher, S. E., et al. (2006), Inverse estimates of anthropogenic CO_2 uptake, transport, and storage by the ocean, *Global Biogeochem. Cycles*, 20, GB2002, doi:10.1029/2005GB002530.
- Millero, F. J., K. Lee, and M. Roche (1998), Distribution of alkalinity in the surface waters of the major oceans, *Mar. Chem.*, 60(1–2), 111–130.
- Naegler, T., and I. Levin (2006), Closing the global radiocarbon budget 1945–2005, *J. Geophys. Res.*, 111, D12311, doi:10.1029/2005JD006758.
- Naegler, T., P. Ciais, K. Rodgers, and I. Levin (2006), Excess radiocarbon constraints on air-sea gas exchange and the uptake of CO_2 by the oceans, *Geophys. Res. Lett.*, 33, L11802, doi:10.1029/2005GL025408.
- Nightingale, P. D., P. S. Liss, and P. Schlosser (2000), Measurements of air-sea gas transfer during an open ocean algal bloom, *Geophys. Res. Lett.*, 27, 2117–2120.

- Orr, J. C., et al. (2001), Estimates of anthropogenic carbon uptake from four three-dimensional global ocean models, *Global Biogeochem. Cycles*, 15, 43–60.
- Peacock, S. (2004), Debate over the ocean bomb radiocarbon sink: Closing the gap, *Global Biogeochem. Cycles*, 18, GB2022, doi:10.1029/2003GB002211.
- Peng, T. S., T. Takahashi, W. S. Broecker, and J. Olafsson (1987), Seasonal variability of carbon dioxide, nutrients and oxygen in the North Atlantic surface water: Observations and a model, *Tellus, Ser. B*, 39, 439–458.
- Rubin, S. I., and R. M. Key (2002), Separating natural and bomb-produced radiocarbon in the ocean: The potential alkalinity method, *Global Biogeochem. Cycles*, 16(4), 1105, doi:10.1029/2001GB001432.
- Sabine, C. L., et al. (2004), The oceanic sink for anthropogenic CO_2 , *Science*, 305, 367–371.
- Sarmiento, J. L., J. C. Orr, and U. Siegenthaler (1992), A perturbation simulation of CO_2 uptake in an ocean general circulation model, *J. Geophys. Res.*, 97, 3621–3645.
- Takahashi, T., et al. (2002), Global sea-air CO_2 flux based on climatological surface ocean pCO_2 , and seasonal biological and temperature effects, *Deep Sea Res., Part II*, 49(9–10), 1601–1622.
- Tans, P. P., I. Y. Fung, and T. Takahashi (1990), Observational constraints on the global atmospheric CO_2 budget, *Science*, 247, 1431–1438.
- Wanninkhof, R. (1992), Relationship between wind-speed and gas-exchange over the ocean, *J. Geophys. Res.*, 97, 7373–7382.
- Wanninkhof, R., J. R. Ledwell, and W. S. Broecker (1985), Gas-exchange wind-speed relation measured with sulfur-hexafluoride on a lake, *Science*, 227, 1224–1226.
- Zhang, J., P. D. Quay, and D. O. Wilbur (1995), Carbon-isotope fractionation during gas-water exchange and dissolution of CO_2 , *Geochim. Cosmochim. Acta*, 59, 107–114.

E. Gloor, Earth and Biosphere Institute, University of Leeds, Leeds LS2 9JT, UK.

A. R. Jacobson and C. Sweeney, Earth System Research Laboratory, NOAA, Boulder, CO 80305, USA. (colm.sweeney@noaa.gov)

R. M. Key and J. L. Sarmiento, Atmospheric and Ocean Sciences Program, Princeton University, Princeton, NJ 08540, USA.

G. McKinley, Department of Atmospheric and Oceanic Sciences, University of Wisconsin-Madison, Madison, WI 53706, USA.

R. Wanninkhof, Atlantic Oceanographic and Meteorological Laboratory, NOAA, Miami, FL 33149, USA.